

# A NEW DERIVATION OF HORIZONTAL TWO DIMENSIONAL DEPTH AVERAGED MOMENTUM EQUATION AND CONTINUITY EQUATION, WHICH INCLUDE TOTAL EFFECT OF POROSITY INSIDE THE VEGETATION

N. A. K. NANDASENA<sup>1</sup>, Norio TANAKA<sup>2</sup> and Toshimitsu TAKAGI<sup>3</sup>

<sup>1</sup>Member of JSCE, B.Sc.Eng (Hons), Graduate School of Science and Engineering, Saitama University (255 Shimo-okubo, Sakura-ku, Saitama 338-8570, Japan)

<sup>2</sup>Member of JSCE, Dr. of Eng., Assoc. Professor, Graduate School of Science and Engineering, Saitama University (255 Shimo-okubo, Sakura-ku, Saitama 338-8570, Japan)

<sup>3</sup>Member of JSCE, Dr. of Eng., Numerical Simulation Department, INA Corporation (1-44-10 Sekiguchi, Bunkyo-ku, Tokyo 112-8668, Japan)

Porosity effects on the hydrodynamic equations are minimal in comparison with other resistance forces like drag and inertia that generated by water flow through vegetation in case of sparsely grown forests. However, in case of densely grown vegetation that have lowest porosity (high blockage) can impose considerable effects on final outcomes. Horizontal two-dimensional depth averaged momentum and continuity equations were derived in first principles with porosity enhancement and it was noticed that new derivations showed considerable contrast with early practiced equations. Two-dimensional numerical simulations were employed to show difference between the results of new and previous equations. It was found that, newly derived equations predicted maximum current velocity was higher than previous equations, maximum water depth was less than previous equations at mid and front of the forest, but maximum water depth was higher than previous equations at behind the forest.

*Key Words* : Porosity, derivation, hydrodynamic behavior, depth averaged momentum and continuity

## 1. INTRODUCTION

Two-dimensional depth averaged equations have been refined to include the hydrodynamic force effects (like drag, inertia, viscous, etc.), induced by vegetation and blockage effect of the mass fluxes through the vegetation. Harada et al.<sup>1)</sup> used Morison's equation for evaluating force in the unsteady flow through the vegetation. The equation included itself that acting force in unsteady flow was the total of drag force and inertia force. Two-dimensional depth averaged equations with porosity modification were employed by Wu et al.<sup>2)</sup> to elucidate the effects of mangrove forests on the flow structures in estuaries. They found that the drag force induced by mangrove tree played a key role in the hydrodynamic process, and blockage from the mangrove trees also played an important role when the porosity of the mangrove trees was less than 0.8. Two dimensional depth averaged equations with porosity modification were employed by Tanaka et al.<sup>3)</sup> to elucidate the effects of coastal vegetation on tsunami Protection. Above study proved, the effect

of porosity generated due to vegetation could become major influence to the final results in case of densely grown forest structures. However, they had not fundamentally discussed the derivation of equations and especially terms of porosity interacted with each of mathematical terms in the system of equations. In this paper, two dimensional depth averaged continuity and momentum equations were derived in first principles and paid keen attention to the porosity term.

## 2. MATERIALS AND METHODS

### (1) Derivation of governing equations in first principles

Both continuity and momentum equations were derived in first principles. Porosity inside the vegetation per unit area is defined below. Vegetation assumed to be vertical cylindrical structures in mathematical equations. Let us take the tree diameter as  $d$  and number of trees per unit area is  $m$ . Porosity based on surface area can be written as (or total water area occupied inside the control

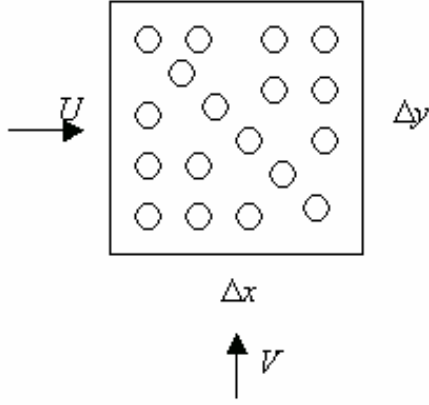


Fig. 1 Sketch of control area with vegetation

Table 1 Nomenclature

Notation	
$U$	Depth averaged flow velocity in $x$ direction
$V$	Depth averaged flow velocity in $y$ direction
$h$	Water depth on bed
$z$	Land elevation measured from the datum
$\theta$	Porosity (0-1)
$\sum_{i=1}^k f_x, \sum_{i=1}^k f_y$	Force induced by vegetation per unit area in $x$ and $y$ direction, respectively. (drag, inertia, viscous, etc.)
$\sum_{i=1}^k \tau_x, \sum_{i=1}^k \tau_y$	Forces induced by other means per unit area in $x$ and $y$ direction, respectively. (bed roughness, wind, Coriolis, etc.)
$\rho$	Density of fluid
$\lambda$	Bed slope
$g$	Gravitational acceleration

area) as  $\Delta x \Delta y \theta$ .

Where,  $\theta = 1 - \pi \frac{d^2}{4} m$

Continuity equation for concerned control volume (without vegetation, control volume is  $\Delta x \Delta y h$ ) can be derived as follows. Effect of porosity taken into account, new control area and control volume become  $\theta \Delta x \Delta y$  and  $\theta \Delta x \Delta y h$ , respectively.

Considering continuity of flow,

$$\begin{aligned} \theta \Delta x \Delta y \Delta h = & (U \sqrt{\theta} \Delta y h - (U \sqrt{\theta} \Delta y h + \frac{\partial(U \sqrt{\theta} \Delta y h)}{\partial x} \Delta x) \\ & + V \sqrt{\theta} \Delta x h - (V \sqrt{\theta} \Delta x h + \frac{\partial(V \sqrt{\theta} \Delta x h)}{\partial y} \Delta y)) \Delta t \end{aligned}$$

By rearranging above,

$$\sqrt{\theta} \frac{\partial h}{\partial t} + \frac{\partial(Uh)}{\partial x} + \frac{\partial(Vh)}{\partial y} = 0 \quad (1)$$

Momentum equation along  $x$  direction is derived

below. It is assumed that hydrostatic pressure distribution exists in the flow.

$$\begin{aligned} \frac{\partial(\theta \Delta x \Delta y h \rho U)}{\partial t} = & - \frac{\partial(\sqrt{\theta} \Delta y h U \rho U)}{\partial x} \Delta x - \frac{\partial(\sqrt{\theta} \Delta x h V \rho U)}{\partial y} \Delta y \\ & - \left[ \frac{\partial(h \rho g)}{\partial x} \Delta x \right] \sqrt{\theta} \Delta y h + \theta \Delta x \Delta y h \rho g \sin(\lambda) \\ & - \sum_{i=1}^k \tau_x \theta \Delta x \Delta y - \sum_{i=1}^k f_x \theta \Delta x \Delta y \\ & \sqrt{\theta} \frac{\partial(hU)}{\partial t} + \frac{\partial(hU^2)}{\partial x} + \frac{\partial(hUV)}{\partial y} + gh \frac{\partial h}{\partial x} + \sqrt{\theta} gh \frac{\partial z}{\partial x} \\ & + \frac{\sqrt{\theta}}{\rho} \sum_{i=1}^k \tau_x + \frac{\sqrt{\theta}}{\rho} \sum_{i=1}^k f_x = 0 \end{aligned} \quad (2)$$

Similarly momentum equation in  $y$  direction becomes,

$$\begin{aligned} \sqrt{\theta} \frac{\partial(hV)}{\partial t} + \frac{\partial(hUV)}{\partial x} + \frac{\partial(hV^2)}{\partial y} + gh \frac{\partial h}{\partial y} + \sqrt{\theta} gh \frac{\partial z}{\partial y} \\ + \frac{\sqrt{\theta}}{\rho} \sum_{i=1}^k \tau_y + \frac{\sqrt{\theta}}{\rho} \sum_{i=1}^k f_y = 0 \end{aligned} \quad (3)$$

Equations (1), (2) and (3) are the newly derived governing equations with total porosity effect, namely two-dimensional depth averaged continuity, momentum in  $x$  direction and momentum in  $y$  direction respectively. To compare newly derived governing equations (hereafter **new** equations) with previously employed equations (hereafter **previous** equations), the equations used by Tanaka et al.<sup>3)</sup> are replaced below. The equations adopted by Wu et al.<sup>2)</sup> were also similar to this, but different symbols were employed.

$$\theta \frac{\partial h}{\partial t} + \frac{\partial M}{\partial y} + \frac{\partial N}{\partial x} = 0 \quad (4)$$

$$\frac{\partial M}{\partial t} + \frac{\partial(UM)}{\partial x} + \frac{\partial(VM)}{\partial y} + gh \frac{\partial H}{\partial x} + \theta_0 \frac{\tau_{xb}}{\rho} + \frac{f_x}{\rho} = 0 \quad (5)$$

$$\frac{\partial N}{\partial t} + \frac{\partial(UN)}{\partial x} + \frac{\partial(VN)}{\partial y} + gh \frac{\partial H}{\partial y} + \theta_0 \frac{\tau_{yb}}{\rho} + \frac{f_y}{\rho} = 0 \quad (6)$$

where,  $M = Uh$ ,  $N = Vh$ ,  $H = h + z$ ,  $\tau_{xb}$ ,  $\tau_{yb}$  = bed shear stress components in  $x$  and  $y$  directions respectively,  $f_x$ ,  $f_y$  = drag force per unit area in  $x$  and  $y$  directions respectively,  $\theta_0$  = porosity in area at bed. Equations (1) and (4) showed similar order except porosity effect to temporal variation of water depth but in new momentum equations (2) and (3), many terms were affected by porosity improvement. Temporal variation of momentum and

spatial variation of water depth were modified by porosity. Moreover, resistance forces imposed by vegetation to water flow were rectified according to reality such that forces were taken by only total area deducted the area occupied by vegetation (i.e. true water area), this fact was not considered in Wu et al.<sup>2)</sup> and Tanaka et al.<sup>3)</sup>.

## (2) Mathematical model

In order to substantiate the difference between the results of both previous and new governing equations to which numerical simulations were undertaken with two type of coastal vegetations namely *Cocos nucifera* and *Pandanus odoratissimus*, those have different vegetation characteristics.

### a) Simplification of vegetation structure for numerical modelling

Mathematical models haven't been fully developed so far to elucidate total hydrodynamic behavior of water flow through vegetation. Main reason is that the complex nature of tree structure, In order to model, we assume tree structure can be treated as a cylindrical structure at which additions and improvements are included to interpret the effect of aerial roots, stem, branches and leaves. Tanaka et al.<sup>3)</sup> used coefficients  $\alpha$  and  $\beta$  to interpret the variation of tree structure into mathematical computation.

$\alpha(z)$  = Additional coefficient for expressing vertical tree structure

$\beta(z)$  = Additional coefficient for representing effect of leaves

Depth averaged diameter with additional improvements by depth averaged  $\alpha\beta$  at height  $h$ , is defined,

$$d = D_{ref} \alpha\beta \text{ and } D_{ref} \text{ is reference diameter at 1.2m.}$$

$$\text{where, } \alpha\beta = \int_0^h \alpha(z)\beta(z)dz$$

$\beta$  was taken as 1.25 referring to the previous research<sup>4)</sup>. Fig. 2 shows the variation of depth averaged porosity with tree height. *Pandanus* shows lowest porosity at the bottom of the tree and gradually it increases with height. This type of vegetation has complex spread root structure. Hence they claim higher projection area resulting higher blockage effect and higher drag resistance to flow at low water depths. In case of *Cocos* has uniform porosity variation with tree height, this is because, *Cocos* has more or less constant diameter along the tree height and due to their large spacing, porosity effect is negligible (porosity varies 0.997 to 0.998) compares to *Pandanus*. For the simulation, drag and

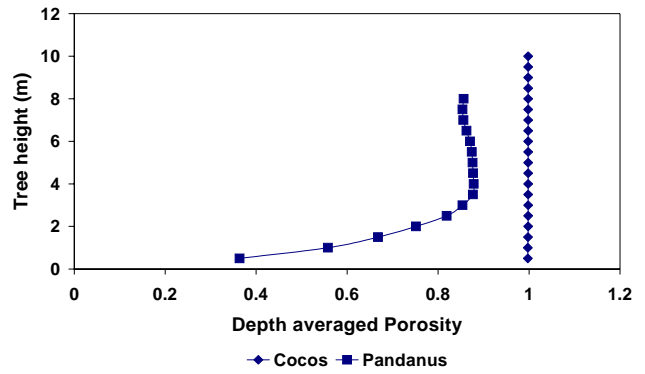


Fig. 2 Variation of depth averaged porosity with tree height

Table 2 Vegetation characteristics

Species	Reference diameter at 1.2m height (m)	Spacing (m)	Density (no. of trees/m <sup>2</sup> )
<i>Cocos</i>	0.35	7	0.02
<i>Pandanus</i>	0.15	1	1

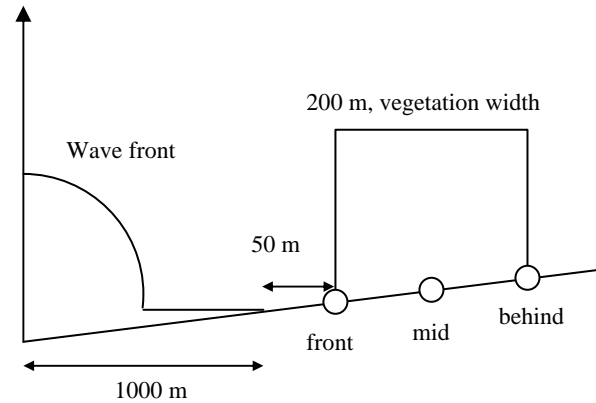


Fig. 3 Schematic diagram of bed profile

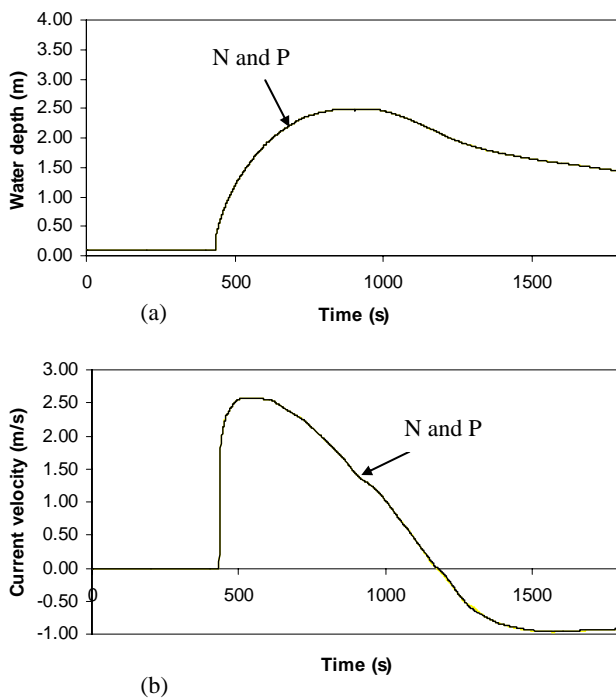
inertia forces were considered to have coefficient of drag,  $C_d$  varied from 1 to 1.5 according to the spacing of the aerial roots<sup>3), 5), 6)</sup> and coefficient of inertia,  $C_M$  was taken as 2.0 referring to cylindrical shape of the tree. Table 2 shows the vegetation characteristics.

### b) Input parameters to simulation

Fig. 3 shows the schematic sketch of simple topography that selected for the simulation. Bed slope was selected to 1:1000, very mild slope, which helps to understand effect of vegetation on water flow without integrating slope effect much. Distance from mean zero sea water level to front face of the vegetation was selected 50 m and additional 1000m was selected from start-boundary to mean zero sea water level to minimize the boundary effects to calculations.

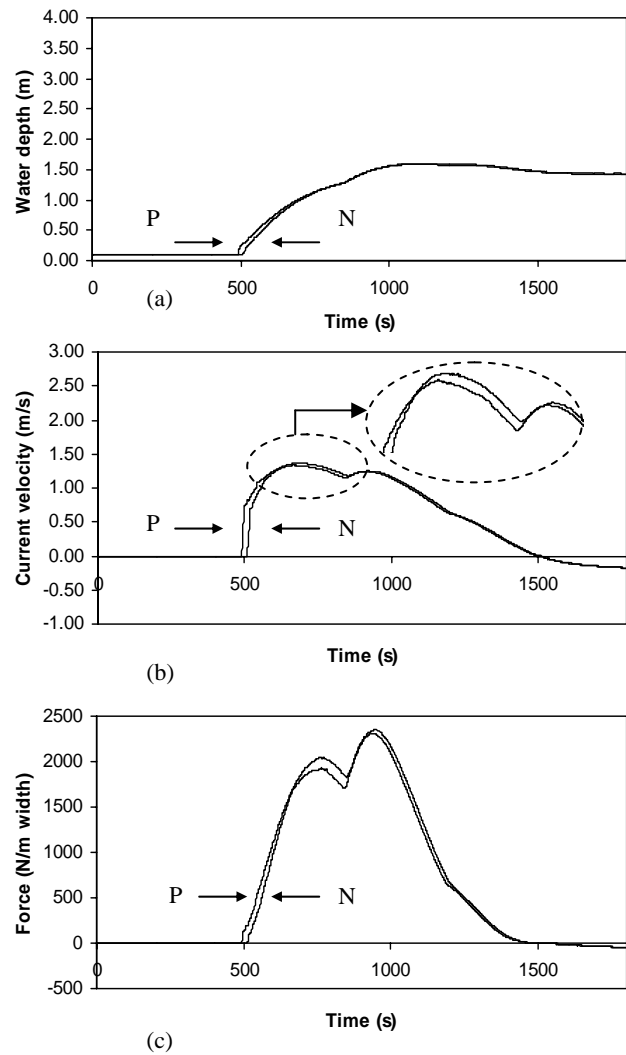
Vegetation width was 200m. Coefficient of Manning roughness was selected to 0.025 to interpret the bed resistance. Selected sin wave (similar to tsunami wave) for the simulation had 30 min period and including both forward and backward fluxes to understand the behavior of outcomes of both in and out flow. Selected  $\Delta x, \Delta y, \Delta t$  values for the simulation were 5m, 5m and 0.025s respectively to make the simulation stable. Temporal variation of currents and water depths in front, mid and behind the vegetation were recorded at every second. Furthermore maximum horizontal run up behind the vegetation were recorded for each species respectively.

### 3. RESULTS AND DISCUSSION



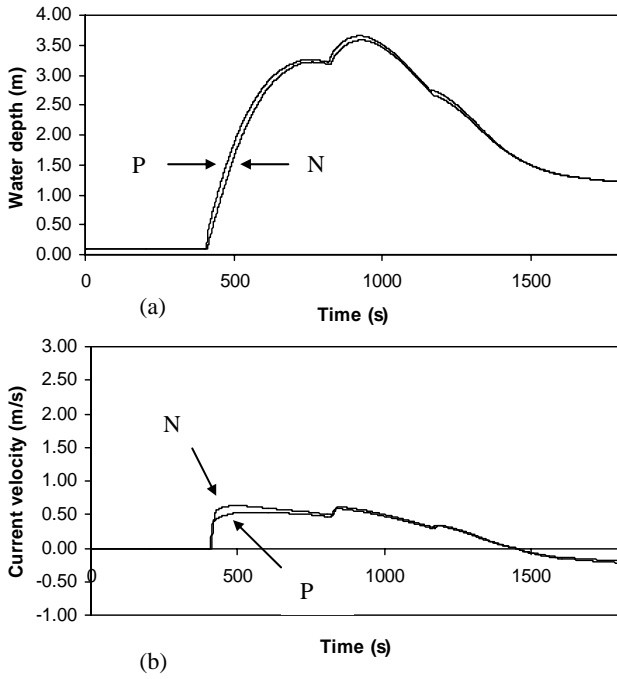
**Fig. 4** Temporal variation of (a) water depth (b) current velocity behind the *Cocos* vegetation for new (N) and previous (P) equations

Fig. 4 (a) and (b) shows the temporal variation of water depth and current velocity behind the *Cocos* forest for new and previous equations respectively. *Cocos* specie was selected to check the high sensitivity of newly derived equation at very high porosity (i.e. sparsely grown vegetation), (as we know at low porosity, there must be effect.) However both results were coincided and this was similar to without vegetation condition. This is because, porosity of *Cocos* was very high and effects to governing equations were negligible and hence equations couldn't distinguish the results. Same trends were observed at in front and mid of the vegetation. Fig. 5 (a) and (b) shows the temporal



**Fig. 5** Temporal variation of (a) water depth, (b) current velocity, (c) hydraulic force behind the *Pandanus* vegetation for new (N) and previous (P) equations

variation of water depth and current velocity behind the *Pandanus* forest for new and previous equations, respectively. It was observed that in Fig. 5(a), new water depths were slightly shifted forward in comparison with previous water depths until water level rose to 1.00m. This was due to low porosity that leads to high blockage at the bottom of *Pandanus* forest resulted by dense root structures. New maximum current velocity was slightly higher than the previous maximum current velocity in Fig. 5 (b). Hydraulic force was expressed as a product of fluid density, the inundation depth and the square of current velocity, and used for estimating the damage of structures behind the forest<sup>7</sup>. Fig. 5 (c) shows the hydraulic force variation per unit width just behind the forest. It was observed new equations generated forces were shifted forward slightly up to 1500 N/m and maximum force was higher than previous equations. Fig. 6 shows the temporal variation of (a) water depth (b) current mid of the *Pandanus* forest



**Fig. 6** Temporal variation of (a) water depth (b) current velocity mid of the *Pandanus* vegetation for new (N) and previous (P) equations

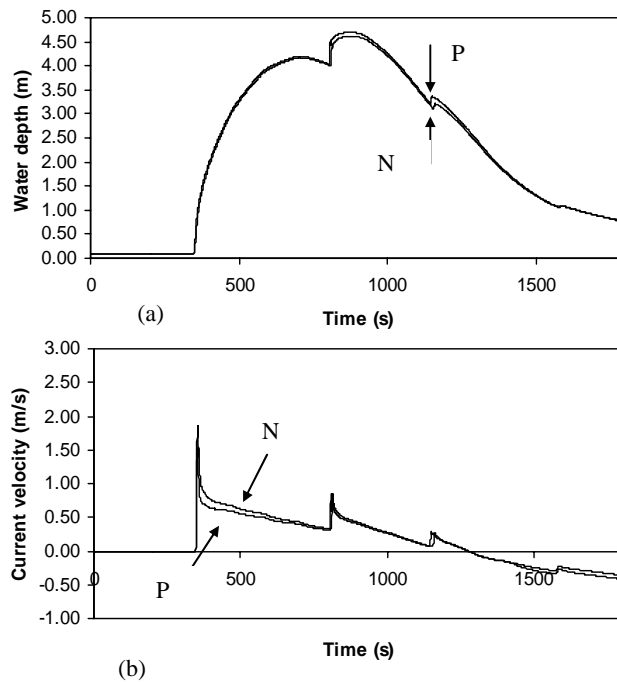


**Fig. 7** Temporal variation of (a) water depth (b) current velocity front of the *Pandanus* vegetation for new (N) and previous (P) equations

for new and previous equations. New water depths were slightly less than previous water depths this resulted high current velocities from new equations. In mid of the forest, there was no initial shifting of new values which was showed in Fig 6. Fig. 7 (a) and (b) shows the temporal variation of water depth

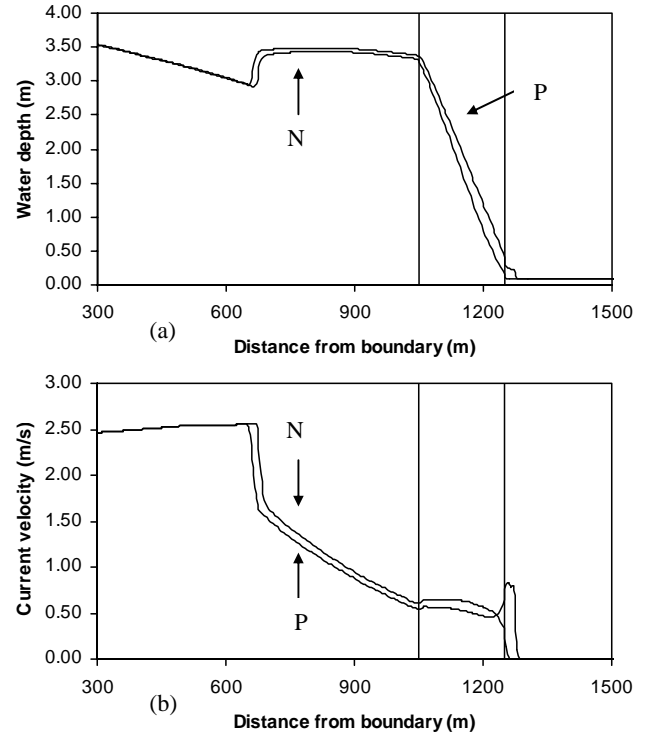


**Fig 8** Spatial variation of (a) water depth (b) current velocity along the bed at 8.5 min including *Pandanus* vegetation (vegetation boundaries are shown by vertical lines) for new (N) and previous (P) equations

and current velocity in front of the *Pandanus* forest for new and previous equations respectively. New equations generated slightly low water depths in front of the forest and this resulted slightly high current velocities compare to previous results. Fig. 7(b) shows initial rising of current velocity, was due to first collision of waterfront on the front face of the vegetation. Following two peaks were due to repelled waves re-reflection at the start boundary. Fig. 8 shows spatial variation of (a) water depth (b) current velocity along the bed including vegetation strip at 8.5 min at which waterfront just exposed to behind the forest. New water depths were slightly less than the previous water depths and which resulting increment of current velocities from new equations. But when waterfront passed just before end boundary, previous current velocities accelerated before new current velocities magnified that led to delay of water reached to behind the forest calculated by new equations than previous equations.

It was learnt by above results, comparison of both new and previous equations were extremely depend on the input parameters selected. However for further comprehension, important simulations results were tabulated in advance which elucidate change of rate of maximum value (hereafter CRMV) defined as follows.

$$\text{CRMV} = \frac{(\text{max. val. of new eqs.} - \text{max. val. of previous eqs.}) \%}{(\text{max. value of previous equations})}$$

**Table 3** Percentage of CRMV of current velocity

Species	Front%	Mid%	Behind%
<i>Cocos</i>	0	0	0
<i>Pandanus</i>	20.8	10.3	1.5

**Table 4** Percentage of CRMV of water depth

Species	Front%	Mid%	Behind%
<i>Cocos</i>	0	0	0
<i>Pandanus</i>	-1.7	-1.9	0.6

**Table 5** Percentage of CRMV of horizontal run up, delay time of water reached behind the forest and hydraulic force behind the forest

Species	Run up%	Delay%	Force%
<i>Cocos</i>	0	0	0
<i>Pandanus</i>	0.7	3.9	2.2

Table 3, Table 4 and Table 5 show percentage of CRMV of current velocity, percentage of CRMV of water depth and CRMV of horizontal run up, delay time of water reached behind the forest and hydraulic force behind the forest for *Cocos* and *Pandanus* species respectively. Summarizing the results of above tables respectively, when the porosity gradually reduces (blockage effect increases), according to the study, simulation results can be classified as follows.

- i. Prediction of maximum current velocity from newly derived equations was higher than previous equations at in front, mid and behind the vegetation respectively.
- ii. Prediction of maximum water depth from newly derived equations was less than previous equations at front and mid of the vegetation respectively, but behind the forest it was opposite.
- iii. Prediction of horizontal run-up behind the forest from newly derived equations was higher than previous equations.
- iv. Prediction of delay in arrival time behind the forest from newly derived equations was higher than previous equations.
- v. Prediction of maximum hydraulic force behind the forest from newly derived equations was higher than previous equations.

### 3. CONCLUSIONS

This study indicated that newly derived two-dimensional depth averaged equations have a

significant difference of components in comparison with the equations that have been practiced so far. Also it was convinced that new derivations were tallied with first principles of mathematics and previous governing equations were under proofed. Both previous and newly derived equations couldn't distinguish the outputs in case of high porosity (low blockage) medium. But, when the porosity decreases (blockage increases), effect of blockage on hydrodynamic parameters is fully imposed by newly derived equations. This was proved by increment of current velocity and decrement of water depths ( $\sqrt{\theta}$  is greater than  $\theta$ , as  $0 \leq \theta \leq 1$ ) within the forest.

Our results were confined only to two vegetation species with limited input conditions, So it is imperative to undertake further study with different vegetation types (porosities), forest widths, bed slopes and flow patterns to elucidate the effects of porosity terms attached to newly derived equations in details. Furthermore future study has to be extended to physical modeling to compare the new results with experiment data to understand the validity of new equations.

**ACKNOWLEDGEMENT:** The Authors remind gratefully Professor Roger A. Falconer, Director Hydro environmental Research Center, Cardiff University, United Kingdom of his useful comments on these new derivations. This study is specially funded by the Heiwa Nakajima Foundation.

### REFERENCES

- 1) Harada, K. and Imamura, F.: Experimental study on the resistance by mangrove under the steady flow, Proceeding of the 1<sup>st</sup> Congress of the Asia and Pacific Coastal Engineering, pp.975-984.
- 2) Wu, Y., Falconer, R. A., and Struve, J.: Mathematical modeling of tidal currents in mangrove forests, Environmental Modeling & Software 16, pp.19-29, 2001.
- 3) Tanka, N., Sasaki, Y., Mowjood, M. I. M., Jindasa, K. B. S. N., and Takemura, T.: Effective coastal vegetation species and structures with landform, sand dune and lagoon, for tsunami protection at the Indian Ocean tsunami, 15<sup>th</sup> APD-IAHR Congress, pp.1279-1285, 2006.
- 4) Fukuoka, S. and Fujita K.: Hydraulic effects of luxuriant vegetations on flood floe (in Japanese). Report of PWRI, vol.180(3), pp. 64, 1990.
- 5) Furukawa, K., Wolanski, K. and Mueller, H.: Currents and sediment transport in mangrove forests. Estuarine, Coastal and Shelf Science, vol.44, pp.301-310, 1997.
- 6) Nepf, H. M.: Drag, turbulence, and diffusion in flow through emergent vegetation. Water Resources Research 35(2), pp.479-489, 1999.
- 7) Hatori, T.: On the damage to houses due to tsunamis (In Japanese), Bull. Earthquake Research Inst. Univ. Tokyo, Vol 59, pp.433-439, 1984.

(Received September 30, 2006)